LETTER

A meta-prism for high-efficiency coupling between free space and optical waveguides with different angular momentums

A Letters Journal Exploring the Frontiers of Physics

August 2018

EPL, **123** (2018) 38001 www.epljournal.org
doi: 10.1209/0295-5075/123/38001

A meta-prism for high-efficiency coupling between free space and optical waveguides with different angular momentums

Yichao Xu[1,2], Hongchen Chu[1,2(a)] and Yun Lai[3,1,2(b)]

[1] *College of Physics, Optoelectronics and Energy & Collaborative Innovation Center of Suzhou Nano Science and Technology, Soochow University - Suzhou 215006, China*
[2] *Key Laboratory of Modern Optical Technologies (Soochow University), Education of Ministry & Key Lab of Advanced Optical Manufacturing Technologies of Jiangsu Province - Suzhou 215006, China*
[3] *National Laboratory of Solid State Microstructures, School of Physics, and Collaborative Innovation Center of Advanced Microstructures, Nanjing University - Nanjing 210093, China*

received 11 June 2018; accepted in final form 7 August 2018
published online 3 September 2018

PACS 81.05.Xj – Metamaterials for chiral, bianisotropic and other complex media
PACS 42.79.Gn – Optical waveguides and couplers
PACS 42.25.Bs – Wave propagation, transmission and absorption

Abstract – In this work, we design a type of meta-prism which can provide high-efficiency coupling between free space and optical waveguides at infrared frequencies. The meta-prism is composed of an ABA multilayer structure with a fixed total thickness. By varying the filling ratio of the components, the phase of the transmitted wave can be tuned to almost cover the whole range of $[0, 2\pi]$, while maintaining a robust high transmittance at the same time. Through two examples, we demonstrate the efficient coupling of light into optical waveguides such as metal wires and optical fibers in a noninvasive way. We also demonstrate an approach to generate waveguide modes with different orbital angular momentums. The meta-prism, as a type of compact and efficient optical coupler, may have important applications in nanophotonics and optical communication.

Introduction. – Traditional prisms are widely applied for coupling between free space and optical devices, such as optical and plasmonic waveguides. However, they are excessively bulky in size and suffer from issues like inherent low efficiency, which make them inconvenient for integration into photonic devices [1–3]. Recently, gradient metasurfaces [4–28] have demonstrated a strong ability to manipulate the phase, polarization and amplitude of electromagnetic waves, which lead to novel applications such as flat lens [6–9], enhanced holography [10–12], photonic spin Hall effect [13], cloaking [14–18], coding devices [19,20], etc. Especially, the conversion of propagating waves into surface waves (SWs) or surface plasmon polariton (SPP) along the metasurfaces [21–24] has been theoretically and experimentally demonstrated in the microwave, optical and terahertz regimes.

The physical mechanism of such a wave conversion process lies in the imposing of an additional wave vector to the reflected [21–23] or transmitted [24] waves via the gradient meta-coupler. When the additional wave vector is beyond the wave number in the background medium, the propagating waves will become evanescent waves that propagate along the surface. The original design was based on the manipulation of reflected waves, which lead to relatively low efficiency. Recently, high efficiency has been successfully obtained based on the manipulation of transmitted waves [24].

Very recently, gradient structures (such as tips) have been proposed to convert cylindrical propagating waves (CPWs) into guided waves (GWs) propagating along a waveguide, as shown in fig. 1(a) [25]. Later, noninvasive meta-couplers have also been designed and demonstrated, as shown in fig. 1(b) [26]. However, the CPWs-GWs conversion efficiency in these approaches is still relatively low due to the physical mechanism based on the manipulation of reflected or scattered waves. Moreover, in the infrared frequency regime, the realization of gradient material parameters turns out to be much more difficult for the noninvasive meta-couplers.

In this work, we propose a method to convert cylindrical propagating waves (CPWs) to guided waves (GWs) by

(a) E-mail: hcchu92@stu.suda.edu.cn
(b) E-mail: laiyun@nju.edu.cn

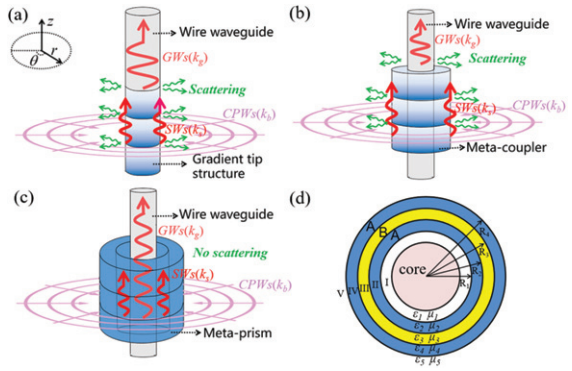

Fig. 1: (Colour online) Schematic graph of (a) reflective gradient tip structures, (b) reflective meta-couplers and (c) transparent meta-prisms. (d) Top view of the transparent meta-prism.

using a highly transparent meta-prism constructed with ABA multilayer structure at infrared frequencies. As shown in fig. 1(c), unlike previous meta-couplers working in the refection geometry [25,26], here, the conversion from CPWs to GWs is based on the tailoring of transmitted waves through the meta-prism. Such a method exhibits the advantage of high efficiency [24] because it is free from the scattering stemming from the discontinuity of two adjacent units of the meta-coupler [27].

For demonstration, we have designed a practical meta-prism that can convert CPWs to GWs that are propagating along a metal wire and an optical fiber at the working wavelength of 1550 nm. Despite the fact that the thickness of each component varies linearly along the axis, the total thickness of the meta-prism is fixed at 760 nm. More interestingly, we demonstrate that such a meta-prism allows the generation of the waveguide modes with different angular momentums, *e.g.*, $m = 0$ and $m = 1$. The numerical results confirmed the conversion efficiency of the meta-prism to be around 61%, which is relatively higher than that of the previous works [26].

Descriptions of the model. – As shown in fig. 1(c), in the CPWs-GWs conversion process, a linearly varying phase shift is generated along the axial direction of the meta-prism (*i.e.*, z-direction). When there exists a phase difference of $\Delta\varphi$ within a distance of L in the z-direction, an additional wave vector $k_s = \Delta\varphi/L$ along the z-direction is imposed on the transmitted waves. Especially, if k_s is larger than the wave number in the background medium k_b, *i.e.*, $k_s > k_b$, the transmitted waves will turn into SWs propagating on the surface of the meta-prism. The driven SWs on the meta-prism can resonantly couple to eigen GWs (with wave vector k_g) on/in the wire waveguides when the condition $k_g = k_s$ is satisfied.

The model of our meta-prism is a gradient cylindrical annulus multi-layer structure surrounding a waveguide as illustrated in fig. 1(c). Here, we consider a 3-layer structure, which contains efficient degrees of freedom for the engineering of the phase and amplitude of transmitted waves through the structure. The meta-prism is of gradient parameters along the z-direction only, therefore the cross-section in $r-\theta$ plane of the model is isotropic. Figure 1(d) shows the cross-section of the whole system, the core and the regions II to IV represent the waveguide and the 3-layer meta-prism, respectively. Region I represents the gap between the waveguide and the meta-prism, and region V represents the background. The inner and outer radii of the region II are R_1 and R_2. The inner and outer radii of the region IV are R_3 and R_4. ε and μ represent the relative permittivity and relative permeability of these layers and the subscripts 1 to 5 represent regions I to V. To design the gradient meta-prism, we first analyze the transmission and scattering of such a homogeneous 3-layer cylindrical annulus.

Without loss of generality, we consider incident CPWs with transverse electric (TE) polarization (with electric fields parallel to the axis of the cylindrical annulus). The electric field in the p-th layer can be expressed as

$$Ep = \sum_{m=-\infty}^{\infty} [A_{m,p}H_m^{(2)}(k_p r) + B_{m,p}H_m^{(1)}(k_p r)]e^{im\theta}\hat{z}, \quad (1)$$

where $H_m^{(1)}$ and $H_m^{(2)}$ are the first and second kinds of the m-th Hankel functions. $A_{m,p}$ and $B_{m,p}$ are the coefficients of inward- and outward-propagating waves in the p-th layer. Especially, $A_{m,V}$ and $A_{m,I}$ denote the coefficients of the incident and transmitted waves and the ratio $S_m = A_{m,I}/A_{m,V}$ is the transmission coefficient of this multilayer cylinder. And $k_p = \sqrt{\varepsilon_p\mu_p}k_0$ is the wave number in the p-th layer, where $k_0 = 2\pi/\lambda_0$ is the wave number in vacuum.

By matching the boundary conditions, we can derive the relationship between the coefficients $A_{m,p}$ and $B_{m,p}$in layer I and layer V [28,29] as

$$\begin{pmatrix} A_{m,I} \\ B_{m,I} \end{pmatrix} = M_m \begin{pmatrix} A_{m,V} \\ B_{m,V} \end{pmatrix}, \quad (2)$$

with $M_m = M_{m,I}M_{m,II}M_{m,III}M_{m,IV}$ and

$$M_{m,p} = \begin{pmatrix} H_m^{(2)}(k_pR_p) & H_m^{(1)}(k_pR_p) \\ \sqrt{\varepsilon_p\mu_{p+1}}H_m^{(2)\prime}(k_pR_p) & \sqrt{\varepsilon_p\mu_{p+1}}H_m^{(1)\prime}(k_pR_p) \end{pmatrix}^{-1} \times \begin{pmatrix} H_m^{(2)}(k_{p+1}R_p) & H_m^{(1)}(k_{p+1}R_p) \\ \sqrt{\varepsilon_{p+1}\mu_p}H_m^{(2)\prime}(k_{p+1}R_p) & \sqrt{\varepsilon_{p+1}\mu_p}H_m^{(1)\prime}(k_{p+1}R_p) \end{pmatrix}.$$

The transmission coefficient can be derived as

$$S_m = A_{m,I}/A_{m,V} = M_m[1,1] - M_m[1,2]M_m[2,1]/M_m[2,2]. \quad (3)$$

From the transmission coefficient S_m, the phase of the transmitted waves φ and the transmittance T can be obtained as $\varphi = \mathrm{Arg}(Sm)$ and $T = |Sm|^2$, respectively.

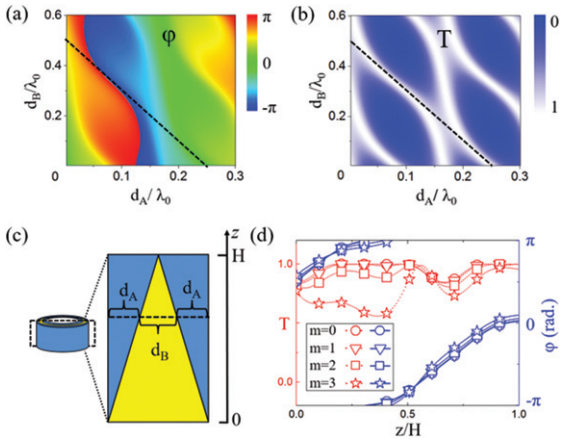

Fig. 2: (Colour online) (a) Transmission phase φ and (b) transmittance T of the ABA-structured dielectric layers as a function of d_A and d_B when $m = 0$. Here, ε_A and ε_B are fixed at 9.3 and 2.3 separately. (c) Cross-section of the meta-prism in the r-z plane (with $d_{A\,\max} = 0.2465\lambda_0$, $d_{B\,\max} = 0.4930\lambda_0$). (d) φ and T of the structure shown in (c) for different angular momentums as a function of z when $R_1 = 0.63\lambda_0$.

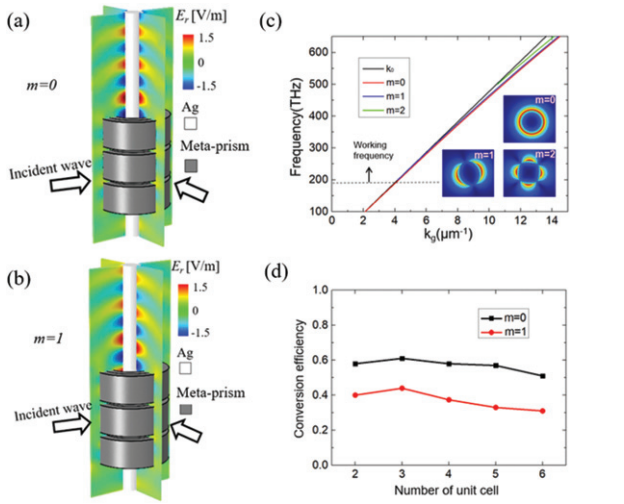

Fig. 3: (Colour online) Snapshots of the radial component of electric-fields E_r distribution for the meta-prism surrounding a silver nanowire under illumination of CPWs with angular momentum (a) $m = 0$ and (b) $m = 1$. (c) Dispersion relations of the SPP modes in the single silver nanowire (with $R_{\rm core} = 0.30\lambda_0$). The insets show the electric-field patterns of the silver nanowire eigenmodes. (d) Calculated conversion efficiency of the meta-prisms for different numbers of unit cells.

Meta-prism design. – Two conditions are required in the design of our meta-prism with high efficiency: the local transmittance T at each point of the meta-prism should be near unity, and the linearly varying phase φ of the transmitted wave should almost cover the range of 2π. Here, we introduce the ABA sandwich structure which can support perfect transmission under normal incidence [30–32], where A and B represent two thin layers of different optical materials (with thicknesses d_A and d_B, relative permittivities ε_A and ε_B and relative permeabilities $\mu_{\rm A} = \mu_B = 1$). With the material parameters fixed, we can still manipulate T and φ by changing d_A and d_B.

For simplicity, here we consider the incident waves with zero angular-momentum quantum number (*i.e.*, $m = 0$). Through numerical analysis of eqs. (2) and (3), we set ε_A and ε_B as 9.3 (GaP) and 2.3 (SiO_2), respectively. These parameters are realizable in the infrared frequency regime. We thus set a working wavelength of $\lambda_0 = 1550\,\text{nm}$ ($f_0 = 193.5\,\text{THz}$) in free space. For the inner radius of the meta-prism, we set $R_1 = 0.63\lambda_0$. φ and T as functions of d_A and d_B are calculated according to eq. (3) and shown in figs. 2(a) and (b), respectively. The black dashed lines in figs. 2(a) and (b) satisfy the equation of $2d_A + d_B = 0.4930\lambda_0$ for all d_A, *i.e.*, when d_A changes from 0 to $0.2465\lambda_0$ and d_B changes from $0.4930\lambda_0$ to 0, the total thickness of the ABA structure is a constant of $0.4930\lambda_0$, *i.e.*, 760 nm, as shown in fig. 2(c). The local transmittance at each point of the structure is near unity, and the linearly varying transmission phase covers a wide range of $76\% \times 2\pi$. The height of the structure is depicted by H. In fig. 2(d), we show the calculated T and φ of the meta-prism for different angular-momentum quantum numbers $m = 0$, 1, 2, 3, respectively. It can be seen that for relatively small angular momentums, such as $m = 0$, 1, 2, the transmittance is near unity and the transmission phase is almost linear and covers a range of $76\% \times 2\pi$. While when the angular momentum increases to $m = 3$, the transmittance drops.

We note that the phase of the transmitted waves φ depicted by the black dashed line does not cover the whole 2π range. Usually, the required linearly varying phase shift can be discretized to simplify the design, and this has been widely applied in metasurfaces design previously [4–28]. If we simplify the meta-prism as several segments with different filling ratios of materials A and B, then it possesses discretized transmission phases that changes along the z-axis. An air gap can be regarded as one segment of the meta-prism with $T = 1$ and $\varphi = 0$. As shown in fig. 3(a), we adopt three unit cells of meta-prisms, where each unit cell is composed of dielectric ABA structure and an air gap. The length of one unit cell is represented by L.

Numerical simulation. – To demonstrate the CPW-GW conversion effect, we perform numerical simulations of a metal wire and an optical fiber by using the finite-element software Comsol Multiphysics.

In the first example, we design a meta-prism for metal wire waveguides. It is known that metal wires can function as efficient waveguides of surface plasmon polaritons (SPPs) in the optical and terahertz regions [33–35]. Here, we consider a silver nanowire waveguide with $\varepsilon = -129.2{+}3.3i$ [36] and radius $R_{\rm core} = 0.30\lambda_0$. We study the surface plasmon modes of this silver nanowire as shown in fig. 3(c) by employing the eigenmode analysis approach based on the finite-element method [37]. The length of

one unit is set to be $L = 0.98\lambda_0$ according to k_g of the eigenmodes at the working frequency $f_0 = 193.5\,\mathrm{THz}$ (*i.e.*, $L = 2\pi/k_g$). Through numerical simulation, we find that the optimized height of the air gap that produces the highest CPWs-GWs conversion efficiency is $0.14L$, and the height of the dielectric ABA structure $H = 0.86L$. The optimized distance from the silver wire to the meta-prism is $d = 0.33\lambda_0$. The incident CPW is excited by given a background electric field $E_b = \sum_{m=-\infty}^{\infty} H_m^{(2)}(k_0 r)e^{im\theta}\hat{z}$ ($m = 0$). The TE-polarized waves are incident onto three units of the meta-prism designed in fig. 2(c). Figure 3(a) shows the snapshots of the radial component of the electric fields E_r under the illumination of CPWs with TE polarization and angular momentum quantum number $m = 0$. Since there is no radial component electric field in the incident waves, the shown E_r represents the GWs induced by the meta-prism. It can be found that the GWs are well confined on the silver nanowire and exponentially decay in the radial direction in free space. Moreover, the simulated wave vector of the converted GWs matches the designed additional wave vector k_s very well. The CPW-GW conversion for the silver nanowire waveguide model is proved.

Furthermore, we have calculated the conversion efficiency, which is defined by $\eta = P_s/P_0$, where P_0 is the time-averaged power flow of the incident CPWs impinging onto the meta-prism and P_s is the power flow carried by the GWs. Here, P_s is calculated by the integration $P_s = \iint_S \mathbf{P}\mathrm{d}\mathbf{S}$, where $\mathbf{P}$ is the time-averaged Poynting vector, and $\mathbf{S}$ is a circular plate with a radius of $1.2\lambda_0$ in the r-θ plane at a distance of λ_0 to the top of the meta-prism. According to the simulation results in fig. 3(a), the conversion efficiency of the gradient meta-prism is found to be 61%, which is significantly higher than the previous meta-coupler working in the reflection geometry (where the efficiency is around 38%) [26].

We note that the calculated conversion efficiency of the optical meta-prism is not so high as that of planar meta-couplers [24], in which the efficiency is reported to be as high as 94%. The reasons are explained in the following. Firstly, the continuous and linearly varying transmission phase provided by the designed optical meta-prism does not cover the 2π range. Secondly, although we have used ABA structure to improve the transmittance of the meta-prism, the local transmittance at each point of the meta-prism is not perfectly unity. Thirdly, unlike the planar case, the whole thickness of the meta-prism is relatively large, and this certainly would decrease the transmittance.

Through analyzing the cases of different angular momentums in fig. 2(d), it is predictable that the meta-prism designed for $m = 0$ incidence can also work under $m = 1$ incidence. Then, we carry out numerical simulations to study the CPWs-GWs conversion effect. Here, $L = 0.99\lambda_0$ and $d = 0.36\lambda_0$ are applied. The simulation result shown in fig. 3(b) clearly demonstrates the CPWs-GWs conversion into a waveguide mode with angular momentum $m = 1$.

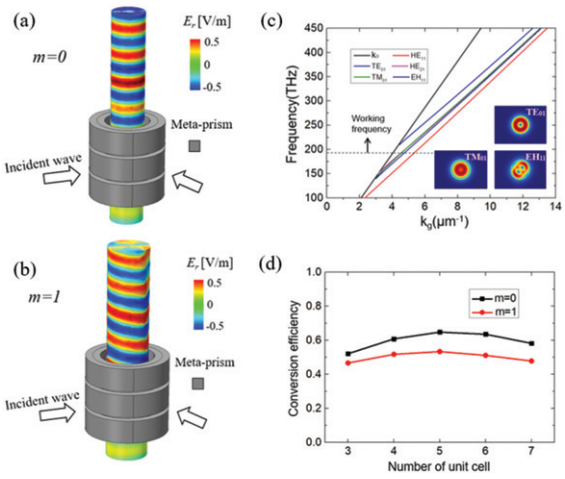

Fig. 4: (Colour online) Snapshots of the radial component of electric fields E_r distribution for the meta-prism surrounding an optical fiber under illumination of CPWs with angular momentum (a) $m = 0$ and (b) $m = 1$. (c) Dispersion relations of the optical fiber (with $R = 0.55\lambda_0$) eigenmodes. The insets show the electric-field patterns of the optical fiber eigenmodes. (d) Calculated conversion efficiency of the meta-prisms for different numbers of unit cells.

We also analyze the influence of the number of unit cells on the conversion efficiency. The efficiency of previous meta-couplers working in the refection geometry decreases rapidly with the increase of unit number due to the scattering stemming from the structure discontinuity of two adjacent units [26,27]. However, the proposed meta-prism is free from this drawback because the converted SWs and GWs propagate along homogeneous waveguides. As shown in fig. 3(d), the calculated conversion efficiency is almost invariable when the number of meta-prisms changes, which is in coincidence with the theoretical analysis.

In the second example, we utilize the meta-prism to convert CPWs to GWs in an optical fiber, which is a dielectric waveguide. By using a similar method as in the metal nanowire case to optimize the parameters of the meta-prism, CPW-GW conversion is realized for different waveguides and angular momentums. For $m = 0$, the parameters of the meta-prism for optical fiber ($\varepsilon = 2.1$, $R_{\mathrm{core}} = 0.55\lambda_0$) are set as $L = 0.89\lambda_0$ and $d = 0.19\lambda_0$. Dispersion relations of the optical fiber (with $R = 0.55\lambda_0$) are shown in fig. 4(c). For $m = 1$, we have applied another set of parameters of $R_{\mathrm{core}} = 0.70\lambda_0$, $L = 0.91\lambda_0$ and $d = 0.21\lambda_0$. The calculated E_r-distributions are shown in figs. 4(a) and (b). TE_{01} and EH_{11} eigenmodes [38] are excited in the case of $m = 0$ and $m = 1$, respectively. Figures 4(a) and (b) demonstrate that the incident CPWs with $m = 0$ and $m = 1$ are efficiently converted to GWs propagating upwards along the optical fiber. The calculated conversion efficiency is almost invariable when the number of meta-prisms changes as shown in fig. 4(d). This example demonstrates that the meta-prism is also applicable to optical fibers.

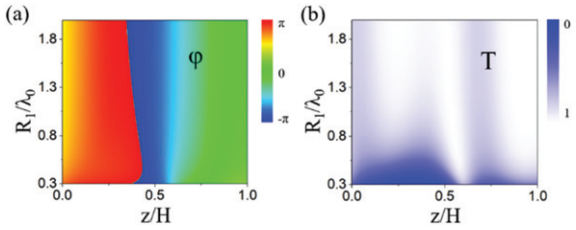

Fig. 5: (Colour online) (a) Transmission phase φ and (b) transmittance T of the meta-prism shown in fig. 2(c) as a function of R_1 when $m = 3$.

Finally, we analyze the influence of the radius on the meta-prism. Since the meta-prism has the geometry of an annular-ring structure, the radius in principle could also affect the conversion efficiency. Here, we select the case of $m = 3$, and calculate the transmission phase and transmittance of the meta-prism as a function of the inner radius R_1 by using eq. (3). The calculation results shown in figs. 5(a) and (b) indicate that the transmission phase has only a small variance for different R_1, which can almost cover a wide range greater than $73\% \times 2\pi$ and is almost always linearly varying with z. However, in fig. 5(b), we find that the transmittance is low when R_1 is small, which coincides with fig. 2(d). Nevertheless, the transmittance increases significantly to over 80% when $R_1 \geq \lambda_0$. Therefore, the designed meta-prism could also apply to incident waves with even larger angular momentums when the radius of the meta-prism is large enough.

Conclusion. – In this paper we have proposed a high-efficiency meta-prism which can convert CPWs in free space to GWs along waveguides. The meta-prism is constructed with ABA multi-layer structure, which can generate transmitted waves with an almost linearly varying phase, *i.e.*, imposing an additional wave vector to the transmitted waves. When the additional wave vector is large enough, the transmitted waves can be coupled to the GWs in the waveguides. For demonstration, we have designed the meta-prism for a silver nanowire and an optical fiber. Relatively high conversion efficiency has been achieved in both cases. Interestingly, the meta-prism applies for different angular momentums, which provides a method to generate GWs with different angular momentums. The meta-prism is made of pure dielectrics and exhibits the advantages of compactness and high efficiency. It can also be extended to two dimensions for the generation of surface waves or guided waves in planar waveguides at infrared frequencies.

* * *

The authors acknowledge financial support from the National Natural Science Foundation of China (NSFC) (61671314) and Priority Academic Program Development of Jiangsu Higher Education Institutions (PAPD).

REFERENCES

[1] Otto A., *Z. Phys.*, **216** (1968) 398.
[2] Berini P., *Adv. Opt. Photonics*, **1** (2009) 484.
[3] Lockyear M. J., Hibbins A. P. and Sambles J. R., *Phys. Rev. Lett.*, **102** (2009) 073901.
[4] Yu N., Genevet P., Kats M. A., Aieta F., Tetienne J., Capasso F. and Gaburro Z., *Science*, **334** (2011) 333.
[5] Ni X., Emani N. K., Kildishev A. V., Boltasseva A. and Shalaev V. M., *Science*, **335** (2012) 427.
[6] Chen X., Huang L., Mühlenbernd H., Li G., Bai B., Tan Q., Jin G., Qiu C. W., Zhang S. and Zentgraf T., *Nat. Commun.*, **3** (2012) 1198.
[7] Lin D., Fan P., Hasman E. and Brongersma M. L., *Science*, **345** (2014) 298.
[8] Khorasaninejad M., Chen W. T., Devlin R. C., Oh J., Zhu A. Y. and Capasso F., *Science*, **352** (2016) 1190.
[9] Wang S., Wu P. C., Su V. C., Lai Y. C., Chu C. H., Chen J. W., Lu S. H., Chen J., Xu B., Kuan C. H., Li T., Zhu S. and Tsai D. P., *Nat. Commun.*, **8** (2017) 187.
[10] Huang L., Chen X., Muhlenbernd H., Zhang H., Chen S., Bai B., Tan Q., Jin G., Cheah K., Qiu C., Li J., Zentgraf T. and Zhang S., *Nat. Commun.*, **4** (2013) 2808.
[11] Ni X., Kildishev A. V. and Shalaev V. M., *Nat. Commun.*, **4** (2013) 2807.
[12] Zheng G., Mühlenbernd H., Kenney M., Li G., Zentgraf T. and Zhang S., *Nat. Nanotechnol.*, **10** (2015) 308.
[13] Yin X., Ye Z., Rho J., Wang Y. and Zhang X., *Science*, **339** (2013) 1405.
[14] Alù A., *Phys. Rev. B*, **80** (2009) 245115.
[15] Zhang J., Lei Mei Z., Ru Zhang W., Yang F. and Jun Cui T., *Appl. Phys. Lett.*, **103** (2013) 151115.
[16] Ni X., Wong Z. J., Mrejen M., Wang Y. and Zhang X., *Science*, **349** (2015) 1310.
[17] Orazbayev B., Mohammadi Estakhri N., Beruete M. and Alu A., *Phys. Rev. B*, **91** (2015) 195444.
[18] Yang Y., Jing L., Zheng B., Hao R., Yin W., Li E., Soukoulis C. M. and Chen H., *Adv. Mater.*, **28** (2016) 6866.
[19] Cui T. J., Qi M. Q., Wan X., Zhao J. and Cheng Q., *Light Sci. Appl.*, **3** (2014) e218.
[20] Li L., Cui T. J., Ji W., Liu S., Ding J., Wan X., Li Y. B., Jiang M., Qiu C. W. and Zhang S., *Nat. Commun.*, **8** (2017) 197.
[21] Sun S., He Q., Xiao S., Xu Q., Li X. and Zhou L., *Nat. Mater.*, **11** (2012) 426.
[22] Sun S., Yang K., Wang C., Juan T., Chen W. T., Liao C. Y., He Q., Xiao S., Kung W., Guo G., Zhou L. and Tsai D. P., *Nano Lett.*, **12** (2012) 6223.
[23] Huang L., Chen X., Bai B., Tan Q., Jin G., Zentgraf T. and Zhang S., *Light Sci. Appl.*, **2** (2013) e70.
[24] Sun W., He Q., Sun S. and Zhou L., *Light Sci. Appl.*, **5** (2016) e16003.
[25] Chu H., Luo J. and Lai Y., *Opt. Lett.*, **41** (2016) 3551.
[26] Chu H., Luo J. and Lai Y., *IEEE Photon. J.*, **9** (2017) 1.

[27] Qu C., Xiao S., Sun S., He Q. and Zhou L., *EPL*, **101** (2013) 54002.
[28] Bai P., Wu Y. and Lai Y., *EPL*, **114** (2016) 28003.
[29] Wang T., Luo J., Gao L., Xu P. and Lai Y., *J. Opt. Soc. Am. B*, **30** (2013) 1878.
[30] Zhou L., Wen W., Chan C. T. and Sheng P., *Phys. Rev. Lett.*, **94** (2005) 243905.
[31] Sun W., He Q., Hao J. and Zhou L., *Opt. Lett.*, **36** (2011) 927.
[32] Song Z., He Q., Xiao S. and Zhou L., *Appl. Phys. Lett.*, **101** (2012) 181110.
[33] Wang K. and Mittleman D. M., *Nature*, **432** (2004) 376.
[34] Wang K. and Mittleman D. M., *Phys. Rev. Lett.*, **96** (2006) 157401.
[35] Lu F. F., Li T., Xu J., Xie Z. D., Li L., Zhu S. N. and Zhu Y. Y., *Opt. Express*, **19** (2011) 2858.
[36] Johnson P. B. and Christy R. W., *Phys. Rev. B*, **6** (1972) 4370.
[37] Sun S., Chen H. T., Zheng W. J. and Guo G. Y., *Opt. Express*, **21** (2013) 14591.
[38] Agrawal G. P., *Fiber-Optic Communication Systems* (Wiley, New York) 2012, Chapt. 2, p. 28.